Chemistry International 6(4) (2020) 168-178

International Scientific Organization
http://iscientific.org/
Chemistry International
www.bosaljournals.com/chemint/

# $TiO_2$-kaolinite nanocomposite prepared from the Jordanian Kaolin clay: Adsorption and thermodynamics of Pb(II) and Cd(II) ions in aqueous solution

**Akl M. Awwad[1]*, Mohammad W. Amer[2] and Marwa M. Al-aqarbeh[3]**

[1]Nanotechnology Department, Royal Scientific Society, Amman, Jordan
[2]Department of Chemistry, College of Science, the University of Jordan, Amman, Jordan
[3]National Agricultural Research Center, Al-Baqa, Jordan
*Corresponding author's E. mail: akl.awwad@yahoo.com

**A R T I C L E I N F O**

**Article type:**
Research article
**Article history:**
Received October 2019
Accepted January 2020
October 2020 Issue
**Keywords:**
$TiO_2$-kaolinite nanocomposite
Adsorption
Pb(II)
Cd(II)
Thermodynamics

**A B S T R A C T**

Metal oxides nanoparticles/clay nanocomposites attractd much attention as an adsorbent for the removal of metal ions. $TiO_2$/kaolinite nanocomposite was prepared from the raw Jordanian kaolin clay and evaluated for the removal of Pb(II) and Cd(II) ions from aqueous solutions through adsorption process. The removal percent (%R) of metal ions was determined as a function of contact time, solution pH, adsorbent dosage and temperature. The maximum adsorption capacity, $q_{max}$ for Pb(II) and Cd(II) ions as evaluated by Langmuir isotherm model were 333.33 mg/g and 250 mg/g, respectively. The prepared $TiO_2$/kaolinite nanocomposite from the Jordanian kaolin clay displayed the main advantage for complete removal of Pb(II) and Cd(II) ions from aqueous solutions by a batch adsorption treatment. In view of promising adsorption efficiency for Pb(II) and Cd(II) ions, the $TiO_2$/kaolinite nanocomposites could possibly be used for the adsorption metal ions form industrial wastewater.



**Capsule Summary:** A novel and eco-friendly natural adsorbent ($TiO_2$/kaolinite nanocomposite) was used for the removal of toxic Pb(II) and Cd(II) ions and the prepared adsorbent from the Jordanian kaolin clay showed promising efficiency for the removal of Pb(II) and Cd(II) ions from aqueous solutions.

**Cite This Article As:** A. M. Awwad, M. W. Amer and M. M. Al-aqarbeh. $TiO_2$-kaolinite nanocomposite prepared from the Jordanian Kaolin clay: Adsorption and thermodynamics of Pb(II) and Cd(II) ions in aqueous solution. Chemistry International 6(4) (2020) 168-178. https://doi.org/10.5281/zenodo.3597558

## INTRODUCTION

Water is one of the most important natural resources in Jordan. In the meantime, water contamination, with heavy toxic metals has become an environmental issue. Different methods and techniques have been developed to remove these heavy toxic metals such as chemical precipitation, ion exchange, electrochemical, membrane separation, electrocoagulation and ion flotation (Mavrow et al., 2003; Verbych et al., 2004; González-Muñoz et al., 2006; Sudilovskiy et al., 2007; Boudrahem et al., 2011; Hossain et al., 2012; Tran et al., 2017; Taseidifar et al., 2017). Green methods using different parts of the plants were also reported in literature as adsorbents for removal of toxic heavy metal ions from water, aqueous solutions and industrial wastewater such as grape stalk waste (Martinez et al., 2006), modified grape stem (Schwantes et al., 2018), *barbadensis* Miller waste leaves powder (Gupta, 2019), *Eriobotrya japonica* leaves (Al-Dujaili et al., 2012), *Ficus carcia* leaves (Farhan et al., 2013), loquat bark (Awwad et al., 2010), *Sophora japonica* pods powder (Amer et al., 2015),

*Moringa oleifera* pods (Oluwaseun et al., 2011), *Terminalia catappa* L. fruit shell (Hervira et al., 2015), *Acacia galpinii* seeds and seed pods (Dube and Chingoma, 2016).

Nowadays, nanomaterials have provided a promising technique for removal of toxic heavy metal ions from water, aqueous solutions and industrial wastewater, due to its low cost-effective, high efficiency, and simple to operate using natural and modified nanomaterial adsorbents for water, aqueous solutions and industrial wastewater such as Alumina-coated carbon nanotubes (Gupta et al., 2011), nanocarbon materials, nanometal particles, and polymer-supported nanoparticles (Wang et al., 2012), titanate/$TiO_2$ added lignin (Fu et al., 2019), nanostructured graphite oxide, silica nanoparticles and silica/graphite oxide composite (Sheet et al., 2014), zero valent silver nanoparticles (Al-Qahtani et al., 2019), carbon-based nanomaterials, zero-valent metal, metal-oxide based nanomaterials, and nanocomposites (Yang et al., 2019), polymer-modified magnetic nanoparticles (Ge et al., 2012), flowerlike α-$Fe_2O_3$ nanostructures (Gao et al., 2012), three-dimensional magnetic graphene oxide foam/$Fe_3O_4$ nanocomposite (Lei et al., 2014), nanocomposite $Fe_3O_4$@$SiO_2$-mPD/SP (Tan et al., 2014), coating $Fe_3O_4$ magnetic nanoparticles with humic acid (Liu et al., 2008), γ-$Fe_2O_3$ nanotubes (Roy and Bhattacharya, 2012 and 2013), surface modified magnetic nanoparticles (Ojemaye et al., 2017), gum Arabic modified magnetic nano-adsorbent (Banerjee et al., 2007), a composite from magnetic nanoparticles ($Fe_3O_4$) capped with cetyltrimethylammonium bromide (Elfeky et al., 2017, Wang et al., 2012; Jin et al., 2012), sulfur-modified magnetic nanoparticles (Jafarinejad et al., 2018), nanostructured kaolinite (Alasadi et al., 2019; Amer and Awwad, 2017), hematite nanoparticles (Grover et al., 2012), $Fe_3O_4$@ montmorillonite composite (Hande et al., 2016), Sawdust-kaolinite composite (Ogbu etal., 2019), porous calcium alginate/graphene oxide composite aerogel (Pan et al., 2018), polyrhodanine-encapsulated magnetic nanoparticles (Song et al., 2011), polyvinyl alcohol-modified kaolinite clay (Unuabonah et al., 2008), chitosan-coated agrillaceow limestone (Zhang et al., 2019), Amino-decorated Zr-based magnetic metal-organic frameworks composites (Zr-MFCs) (Huang et al., 2018), nanocomposites of nanosilica-immobilized-nanopolyaniline and crosslinked nanopolyaniline (Mahmoud et al., 2016), hydroxyapatite/cellulose composite (Cho and Jeong, 2008), kaolinite/smectite natural composite (El-Naggaret al.2019), $Fe_3O_4$/cyclodextrin polymer nanocomposites (Badruddoza et al., 2013) and magnetic cellulose-based beads with embedded chemically modified magnetite nanoparticles and activated Carbon (Luo et al., 2016). Hence, nanocomposites proved to be highly efficient for the removal of metal ions form wastewater (Bhatia and Nath, 2020; D'Cruz et al., 2020; Kefeni and Mamba, 2020; Mukwevho et al., 2020; Yue et al., 2020).

In this study, we report a new, rapid and cost-effective route for the adsorption of Pb(II) and Cd(II) ions from aqueous solution onto $TiO_2$/kaolinite nanocomposite prepared from the natural Jordanian kaolin clay. Chemical treatment of natural Jordanian kaolin clay at ambient temperature produced nanocomposite composed mainly from 1.8 wt.% titanium oxide and 98.0 wt.% kaolinite. Adsorption variables such as pH, contact time, adsorbent dose and concentration are reported. Surface characterization of the composite by X-ray fluorescence (XRF), X-ray diffraction (XRD), Fourier transmission infrared (FTIR) and scanning electron microscope (SEM) were discussed. One of the advantageous of this preparation route of $TiO_2$/kaolinite nanocomposite from the raw Jordanian kaolin clay is the production of a by-product of a red pigment composed mainly from nano-iron oxide (hematite).

## MATERIAL AND METHODS

### Chemical, reagents and materials

Lead nitrate $Pb(NO_3)_2$ and cadmium nitrate $Cd(NO_3)_2$ were analytical grade obtained from Sigma-Aldrich, Germany and used without further purifications. Hydrochloric acid (37%) and sodium hydroxide (NaOH) were obtained Merck, Germany. Kaolin clay sample was obtained from Batin El Ghoul deposits, south Jordan. Distilled and de-ionized water were used in all experimental work.

### Preparation of $TiO_2$/kaolinite nanocomposite

$TiO_2$/kaolinite nanocomposite was prepared as follows: The raw Jordanian kaolin clay samples were mechanically crushed ground and sieved to 350 meshes (particle size < 5μm). 500g of the fine powder was treated with hydrochloric acid (20%) under mechanical stirring for 3h at ambient temperature (27°C) and then left overnight at room temperature. After that, a a red-yellow solution (upper layer) removed by decantation. Afterwards the kaolin particles treated with 10% sodium hydroxide under mechanical stirring for 30min. By decantation, filtration and washing with de-ionized water, a white powder was obtained and dried in an oven at 80°C for 4h. The obtained $TiO_2$/kaolinite nanocomposites powder was subjected to chemical analysis, XRF, XRD and SEM.

### Adsorption experiments

Adsorption of Pb(II) and Cd(II) ions onto $TiO_2$/kaolinite nanocomposite was performed in glass flasks of 250 ml containing 0.5 g of adsorbent mass and 20 ml of metal ions solutions with an initial concentrations ranging between 5 to 80 mg/L. The mixture was shaken (~200 rpm) until the equilibrium was reached using a water shaker bath. Then, the solid phase was separated from the liquid phase by centrifugation (2000 rpm for 10 min) and the concentrations of metal remaining were determined by atomic absorption, The amount of adsorbed Pb(II) and Cd(II) ions onto $TiO_2$/kaolinite nanocomposite was calculated using relations shown in Eqs. 1-2.

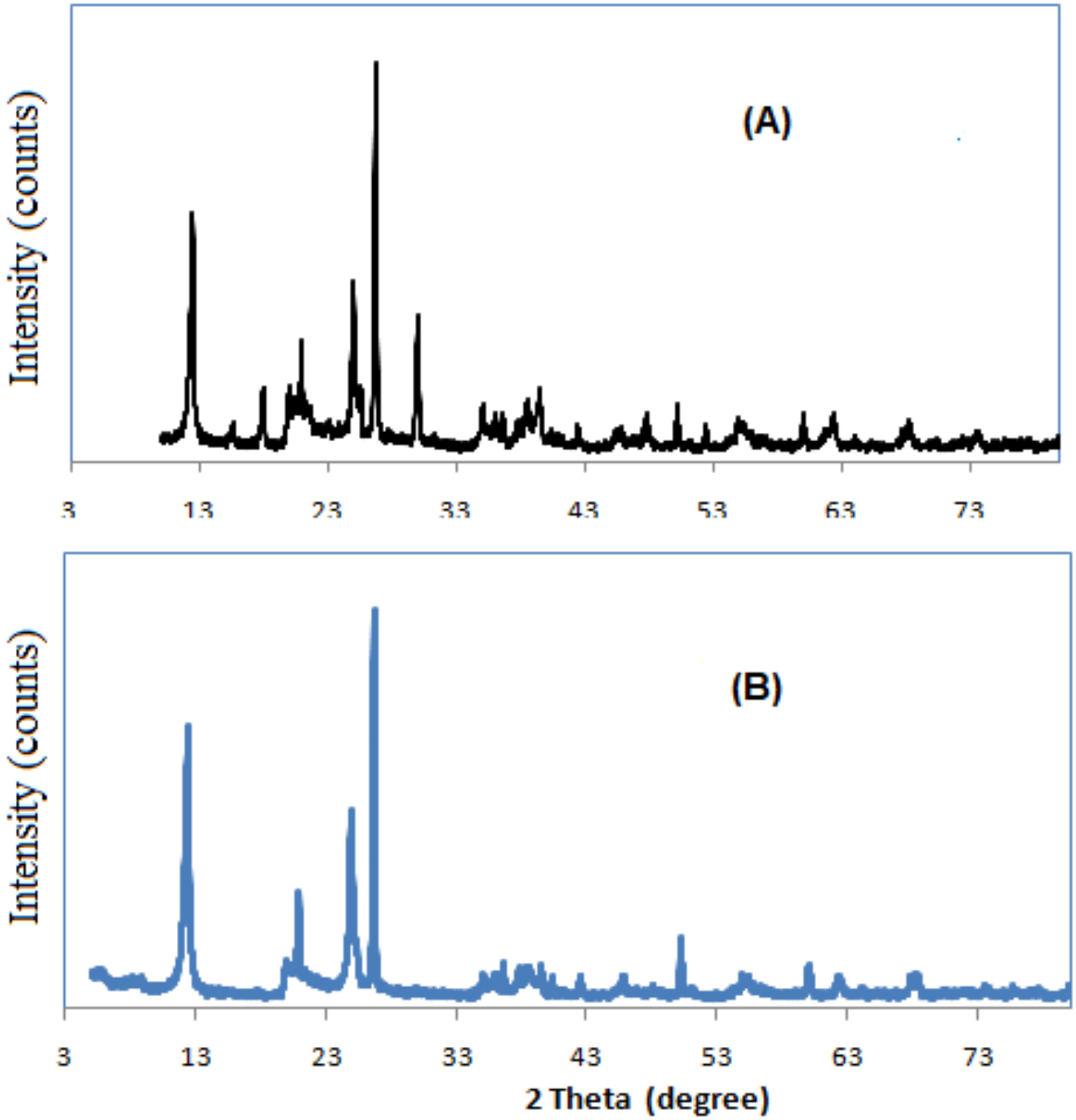


**Fig. 1:** XRD of raw kaolin clay (A) and the prepared TiO2/kaolinite nanocomposite (B)

$$Removal\ (\%) = \frac{C_o - C_e}{C_o}\ x\ 100 \quad (1)$$

$$q_e = \frac{C_o - C_e}{M}\ x\ V \quad (2)$$

Where, $C_o$ (mg/L) is the initial concentration of metal ions and $C_e$ (mg/L) is the equilibrium concentration in aqueous solution. M is the concentration of $TiO_2$/kaolinite nanocomposite, V (L) is the volume of solution. $q_e$ is the amount of adsorbed metal per gram of adsorbent (mg/g) and R% represent the removal percent of metal ions.

Morphology studies

Lead (II) and cadmium (II) ions concentrations were determined by AAS600 atomic spectrophotometer (Schimadzu, Japan), pH measurements were done by WTW pH meter. Fourier transforms infrared spectrophotometer (IR Prestige-21, Schimadzu). $TiO_2$/kaolinite nanocomposite prepared were characterized by X-ray diffractometer,

(XRD-6000, Shimadzu) equipped with Cu K α radiation source (λ =0.154056 nm) using Ni as filter at a setting of 30 kV/30mA. All XRD and XRF data were collected under the experimental conditions in the angular range $3^o \leq 2\theta \leq 80^o$. Scanning electron microscopy (SEM) images were taken using a field emission scanning electron microscopy (Hitachi S4700, 15 kV).

## RESULTS AND DISCUSSION

### XRD analysis

The chemical composition of raw Jordanian kaolin clay and the prepared $TiO_2$/kaolinite nanocomposite by XRF analysis has been determined as: 63.17% $SiO_2$, 23.46% $Al_2O_3$, 2.66% $Fe_2O_3$, 1.56% $TiO_2$, 0.84% CaO, 0.19% MgO, 0.22% $Na_2O$, 0.27% $K_2O$ and 7.43% loss of ignition. The prepared $TiO_2$/kaolinite nanocomposite analysis as: 76.61% $SiO_2$, 19.82% $Al_2O_3$ and 1.8% $TiO_2$. XRF analysis showed that the ratio of $SiO_2/Al_2O_3$ equals 2.69 for raw kaolin clay and 3.87 for the prepared $TiO_2$/kaolinite nanocomposite**.** Results of the X-ray diffraction analysis of raw kaolin clay and the prepared $TiO_2$/kaolinite nanocomposite is shown in Fig. 1. XRF and XRD measurements have shown that the raw kaolin clay composed mainly from kaolinite and metal oxides. HCl and NaOH activities eliminate most metal oxides associated with kaolinite such as calcium, magnesium, potassium, sodium and iron oxides. On the other hand, the prepared $TiO_2$/kaolinite nanocomposite is composed mainly of aluminum silicates and titanium oxide $TiO_2$. This method indicated that the removal of the associated metal materials from the raw kaolin clay by hydrochloric and sodium hydroxide introduced a change into the chemical structure of kaolin clay and increases the surface area and adsorption capacity. XRD analysis of the raw Jordan kaolin clay (A) and the prepared $TiO_2$/kaolinite nanocomposite are illustrated Fig. 1.

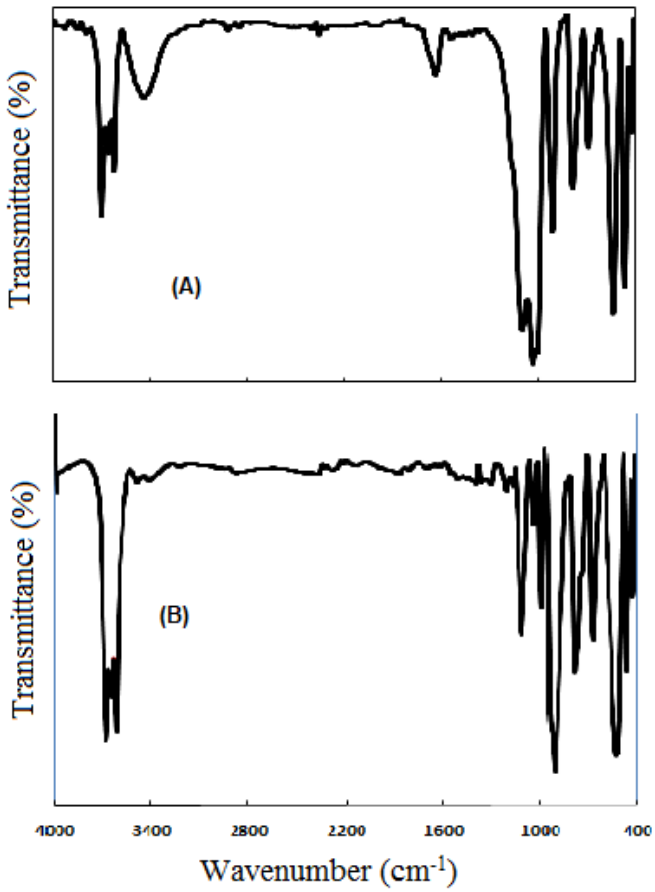


**Fig. 2:** FT-IR of raw kaolin clay (A) and the prepared $TiO_2$/kaolinite nanocomposite (B)

### FT-IR analysis

FT-IR analysis (Fig. 2) showed the hydroxyl stretching vibration bands at 3695 and 3622 $cm^{-1}$, which corresponds to the inner surface –OH stretching vibration of kaolinite. Band at 3486$cm^{-1}$ belongs to the stretching vibration of the outer-surface hydroxyl groups, indicating the presence of kaolinite in raw kaolin clay. The disappearance of bands at 3486 $cm^{-1}$ and 1627 $cm^{-1}$ indicated the acid treatment was effected on these positions. Absorption band at 1627 $cm^{-1}$ assigned for the -OH bending vibration and C=O stretching vibration. The bands at 1110 $cm^{-1}$ and 1026 $cm^{-1}$ moved to 1119 $cm^{-1}$ and 995 $cm^{-1}$ moved in the kaolin clay treated by HCl and sodium hydroxide, corresponding to Si-O bending and stretching vibrations. Absorption band at 914 $cm^{-1}$ corresponds to the Al-O bending vibration. Bands at 540 and 470 $cm^{-1}$ represent to Al-O-Si skeletal vibration. The characteristic hydroxyl (-OH) bands of kaolinite at 3695 $cm^{-1}$ and 3622 $cm^{-1}$ still exists. The intensity of band at 3486$cm^{-1}$ disappears and new band appears at 1119$cm^{-1}$. These results indicated that the hydrogen bonding between the layers of raw kaolin and formation of new hydrogen bonding between the inner–surface hydroxyl groups. The obtained results indicated that the removed associated metal oxides from the raw kaolin clay changed the structure to kaolinite.

### Scanning electron microscopy (SEM) analysis

Scanning electron microscopy (SEM) of raw kaolin clay and the prepared $TiO_2$/kaolinite nanocomposite are illustrated in Fig. 3. SEM of $TiO_2$/kaolinite nanocomposite showed that the platelets shape and the average size 18 nm.

### Effect of contact time

Adsorption of Pb(II) and Cd(II) ions onto $TiO_2$/kaolinite nanocomposite described as a function of contact time, Fig. 4. The adsorbent loading was kept at a constant value of 0.5g and a contact time of 80min. Adsorption capacity equilibrium was achieved between 30-60 min.

**Table 1:** Langmuir and Freundlich parameters

| Langmuir constants | | | |
|---|---|---|---|
| Metal ion | $q_{max}$ (mg/g) | $K_L$(L/mg) | $R^2$ |
| Pb(II) | 333.33 | 0.003 | 0.9999 |
| Cd(II) | 250.14 | 0.004 | 0.9999 |
| Freundlich constants | | | |
| | $K_F$ | n | $R^2$ |
| Pb(II) | 2.26 | 1;493 | 0.9868 |
| Cd(II) | 2.97 | 1.901 | 0.9759 |

**Table 2:** Thermodynamic parameters of Pb(II) and Cd(II ions onto $TiO_2$/ kaolinite nanocomposite

| Metal ion | T/K | $K_D$ | $\Delta G^o$ (KJ/mol) | $\Delta H^o$ (KJ/mol) | $\Delta S^o$ (J/mol) |
|---|---|---|---|---|---|
| Pb(II) | 293 | 5.5 | -4.2 | 11.5 | 53.5 |
| | 303 | 6.42 | -4.7 | | |
| | 313 | 7.44 | -5.2 | | |
| Cd(II) | 293 | 3.4 | -3.7 | 23.5 | 90.4 |
| | 303 | 4.64 | -4.3 | | |
| | 313 | 6.3 | -4.9 | | |

**Effect of pH**

The pH has been identified as one of the most important parameter that is effective on metal adsorption. The effect of pH on the adsorption of Pb(II) and Cd(II) ions onto $TiO_2$/kaolinite nanocomposite was studied at pH 1.0–8.0, Fig.5. The maximum adsorption was observed at pH 5.5-6.0 for PbII) and Cd(II) ions. Therefore, all the remaining adsorption experiments were carried out at this pH value. At highly acidic pH (pH < 3.0), the overall surface charge on the active sites became positive and metal cations and protons compete for binding sites onto TiO2/kaolinite nanocomposite, which results in lower uptake of metal. The adsorbent surface was more negatively charged as the pH solution increased from 5.0 to 6.0.

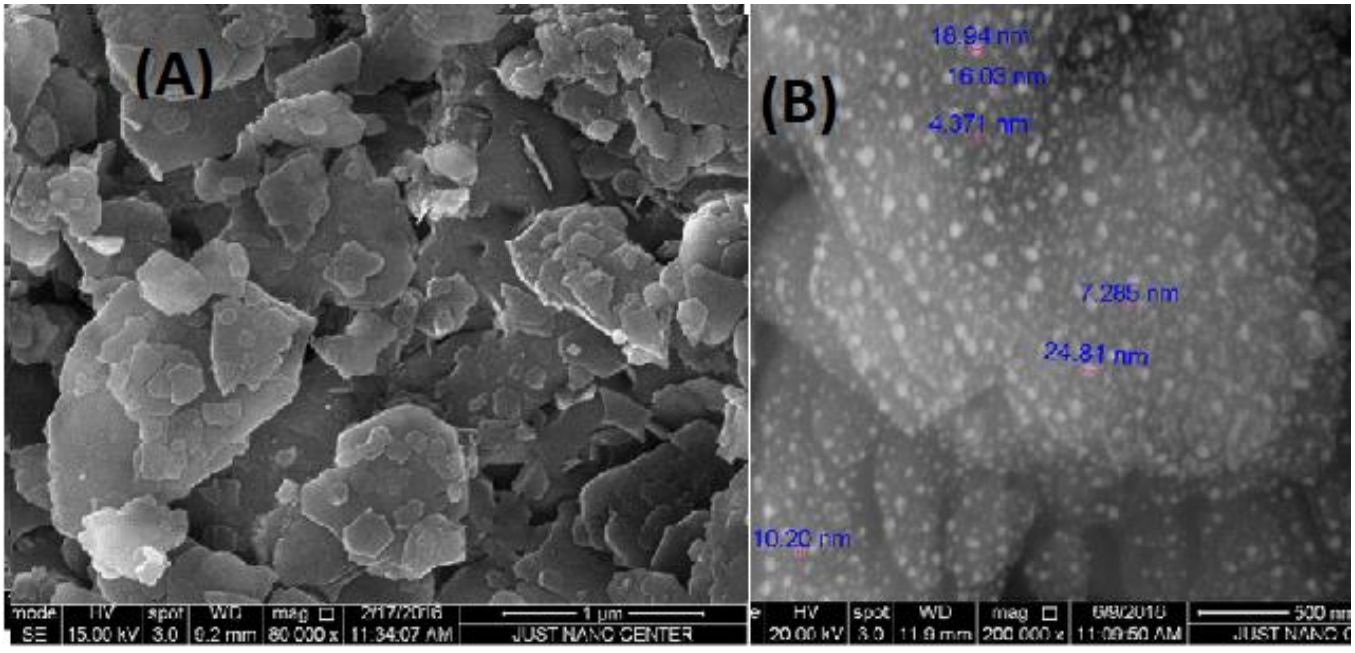


**Fig. 3:** SEM of raw kaolin clay (A), $TiO_2$/kaolinite nanocomposite (B)

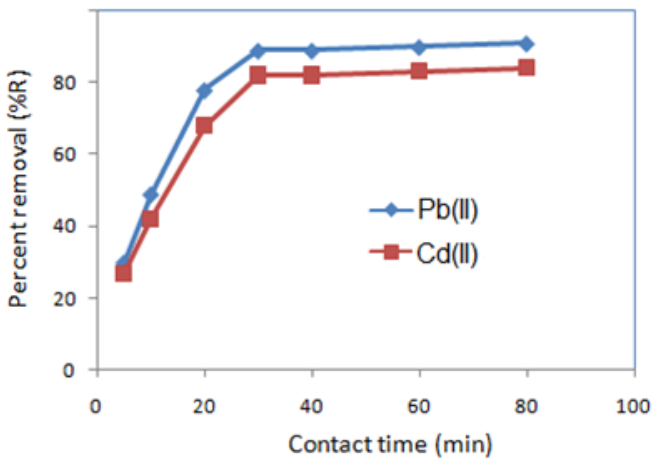


**Fig. 4:** Effect of contact time (min) on percent removal of metal ions

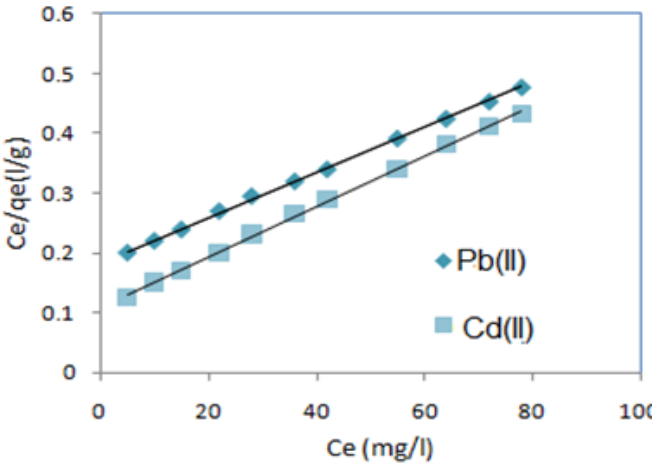


**Fig. 6:** Plot of Langmuir model for adsorption Pb(II) and Cd(II) onto $TiO_2$/kaolinite nanocomposit

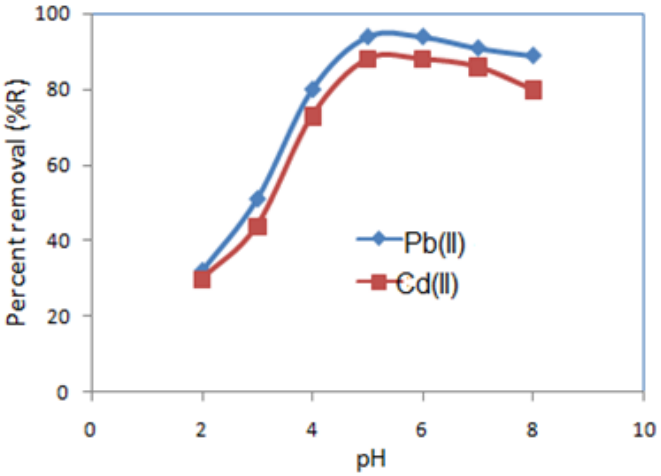


**Fig. 5:** Effect of pH on the percent removal of metal ions

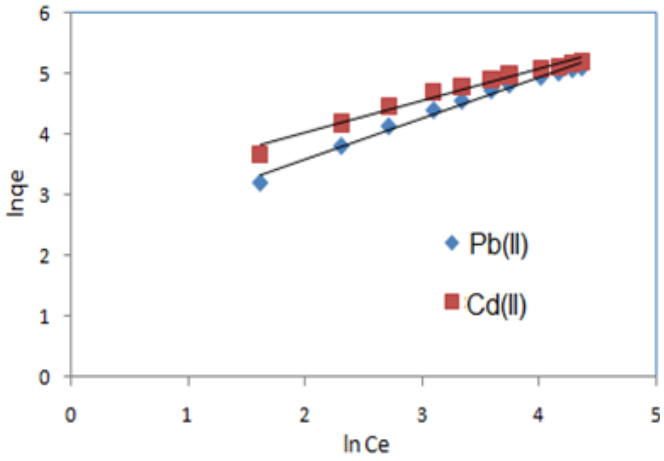


**Fig. 7:** Plot of Freundlich model for adsorption Pb(II) and Cd(II) onto $TiO_2$/kaolinite nanocomposit

**Effect of adsorbent dose**

The adsorption efficiency for Pb(II) and Cd(II ions as a function of adsorbent dosage was investigated. The percentage of the metal adsorption increases with the adsorbentt loading up to 0.5 g/0.1L. This result can be explained by the fact that the adsorpent sites remain unsaturated during the adsorption reaction whereas the number of sites available for adsorption site increases by increasing the adsorbent dose. The maximum adsorption 94.0% for Pb(II) and 88% for Cd(II) was attained at adsorbent dosage, 0.5 g/0.1L. Therefore, the optimum adsorbent dosage was taken as 0.5 g/0.1L for further experiments. As the adsorbent dose increased, more active sites to bind metal ions, thus it results an increase in the adsorption efficiency until saturation.

**Adsorption isotherms**

The linear form of the Langmuir isotherm model is described in Eq. 3 (Langmuir 1918).

$$\frac{C_e}{q_e} = \frac{1}{K_L q_{max}} + \frac{1}{q_{max}} C_e \qquad (3)$$

Where, $K_L$ is the Langmuir constant related to the energy of adsorption and $q_{max}$ is the maximum adsorption capacity (mg/g). Values of Langmuir parameters $q_{max}$ and $K_L$ were calculated from the slope and intercept of the linear plot of $C_e/q_e$ versus $C_e$ as shown in Fig. 6. Values of $q_{max}$, $K_L$ and regression coefficient $R^2$ are listed in Table 1. These values for magnetite/kaolinite nanocomposite adsorbent indicated that Langmuir model describes the adsorption phenomena favarouble. The essential characteristics of the Langmuir isotherm parameters can be used to predict the affinity between the sorbate and sorbent using separation factor or dimensionless equilibrium parameter, $R_L$ expressed in Eq. 4.

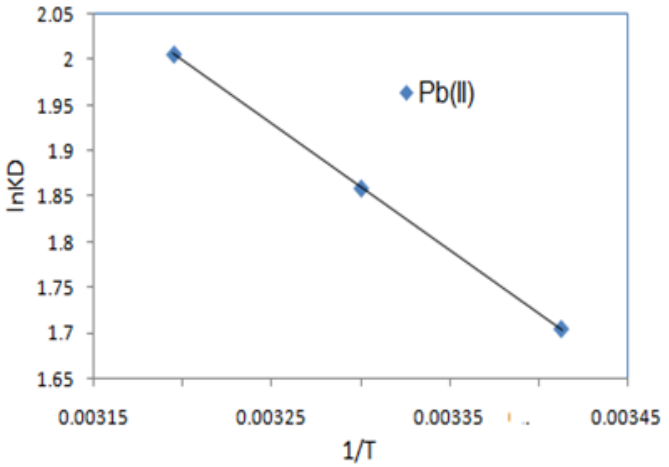


**Fig. 8:** Plot of $\ln K_D$ versus 1/T for adsorption of Pb(II) ions onto $TiO_2$/kaolinite nanocomposite

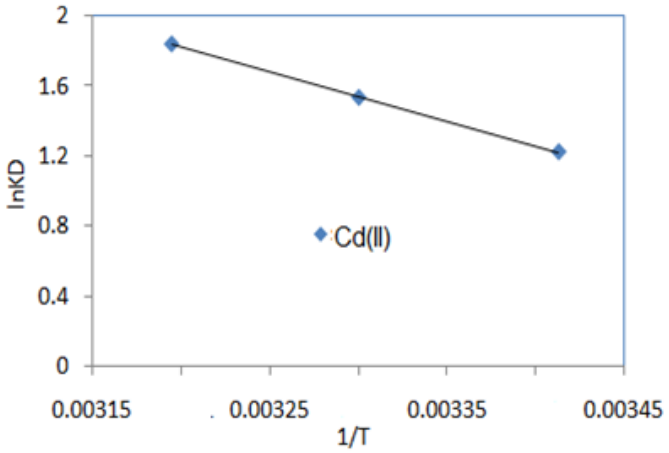


**Fig. 9:** Plot of ln $K_D$ versus 1/T for adsorption of Cd(II) ions onto $TiO_2$/kaolinite nanocomposite

$$R_L = \frac{1}{1+K_L C_e} \quad (4)$$

Where, $K_L$ is the Langmuir constant and $C_e$ is the initial concentration of lead (II) and cadmium (II) ions. The value of separation parameter $R_L$ provides important information about the nature of adsorption. The value of $R_L$ indicated the type of Langmuir isotherm to be irreversible ($R_L$= 0), favorable (0<$R_L$<1), linear ($R_L$=1) or unfavorable ($R_L$>1). The $R_L$ was found to be 0.64-0.88 for concentration of 10–40 mg/L of Pb(II) and Cd(II). They are in the range of 0-1 which indicates the favourable adsorption.

The Freundlich isotherm model is the well-known earliest relationship describing the adsorption process. This model applies to adsorption on heterogeneous surfaces with the interaction between adsorbed molecules and the application of the Freundlich equation also suggests that sorption energy exponentially decreases on completion of the sorption centers of an adsorbent. This isotherm is an empirical equation and can be employed to describe heterogeneous systems and is expressed in Eq. 5 (Freundlich, 1906).

$$lnq_e = lnK_F + \frac{1}{n} lnC_e \quad (5)$$

Where, $K_F$ is the Freundlich constant related to the bonding energy. 1/n is the heterogeneity factor and n (g/L) is a measure of the deviation from linearity of adsorption. Freundlich equilibrium constants were determined from the plot of $\ln q_e$ versus $\ln C_e$, Fig. 7 on the basis of the linear of Freundlich equation. The n value indicates the degree of non-linearity between solution concentration and adsorption as follows: if n=1, then adsorption is linear; if n<1, then adsorption is a chemical process; if n>1, then adsorption is a physical process. The n value in Freundlich equation was found to be 1.49 for Pb(II) and 1.90 for Cd(II) ions, Table 1. Since n lie between 1 and 10, this indicate the physical adsorption lead (II) and cadmium (II) ions onto $TiO_2$/kaolinite nanocomposite. The values of regression coefficients $R^2$ are regarded as a measure of goodness of fit of the experimental data to the isotherm models .

**Thermodynamic study**

Thermodynamic parameters; enthalpy ($\Delta H^o$), entropy ($\Delta S^o$) and Gibbs free energy ($\Delta G^o$) for Pb(II) and Cd(II) ions adsorption onto $TiO_2$/kaolinite nanocomposite were determined as shown in Eq. 6-8.

$$\Delta G^o = \Delta H^o - T\Delta S^o \quad (6)$$

$$lnK_D = -\frac{\Delta H^o}{RT} + \frac{\Delta S^o}{R} \quad (7)$$

$$K_D = \frac{C_a}{C_e} \quad (8)$$

Where, $K_D$ is the equilibrium distribution constant, $C_a$ is mg of adsorbate adsorbed per liter and $C_e$ is the equilibrium concentration of solution, mg/L. The values of enthalpy change ($\Delta H^\circ$) and entropy change ($\Delta S^\circ$) were calculated from the slope and intercept of the plot of $\ln K_D$ vs. 1/T. The calculated values of thermodynamic paramours $\Delta G^\circ$, $\Delta H^\circ$, and $\Delta S^\circ$ for the adsorption of Pb(II) and Cd(II) ions onto $TiO_2$/kaolinite nanocomposite are listed in Table 2. A negative value of the free energy ($\Delta G^\circ$) indicated the spontaneous nature of the adsorption process. It was also noted that the change in free energy, $\Delta G^o$ increase as the temperature increased, indicating more driving force and hence resulting in higher adsorption process. This could be possibly because of activation of more sites on the surface of nanocomposite with increase in temperature or that the energy of adsorption sites has an exponential distribution and a higher temperature enables the energy barrier of adsorption to be overcome. In the physical adsorption the free energy change ($\Delta G^\circ$) ranges from (−20 to 0) kJ/mol and for chemical adsorption it ranges between (−80 and −400)

kJ/mol. The $\Delta G^o$ for Pb(II) and Cd(II) ions adsorption onto $TiO_2$/kaolinite nanocomposite. nanocomposite was in the range of (-3.7 to -5.2) kJ/mol and so the adsorption was predominantly physical adsorption. A positive value of $\Delta S^o$ as 53.5-90.4 J/mol K showed increased randomness at solid solution interface during the adsorption of Pb(II) and Cd(II) ions onto $TiO_2$/kaolinite nanocomposite.

**Efficiency of $TiO_2$/kaolinite nanocomposites**

A comparative of the maximum adsorption capacity, $q_{max}$ of $TiO_2$/kaolinite nanocomposite with those of some other adsorbents reported in literature, for removal of Pb(II) and Cd(II) ions from aqueous solutions is given in Table 3. Differences in $q_{max}$ are due to: Nature and properties of each adsorbent; particle size of adsorbents; surface area; and the main functional groups in the structure of the adsorbent. A comparison with other adsorbents indicated a high Pb(II) and Cd(II) ions adsorption capacity of $TiO_2$/kaolinite nanocomposite prepared by simple, economic and low-cost natural kaolin clay, Table 3. In view of promising efficiency of $TiO_2$/kaolinite nanocomposites for the adsorption of Pb(II) and Cd(II) ions and in comparison to reported studies (Chen et al., 2020; Chowdhury et al., 2020; Ghorbani et al., 2020; Kamari and Shahbazi, 2020; Saeedi-Jurkuyeh et al., 2020; Shahzad et al., 2020; Sheydaei et al., 2020), the nanocomposites have potential to remove metal ions from wastewater.

**CONCLUSIONS**

The experimental investigation concluded that $TiO_2$/kaolinite nanocomposite could be used as potential adsorbent for removal of Pb(II) and Cd(II) ions from aqueous solutions. The batch adsorption parameters: pH of solution, adsorbent dose, contact time, initial metal concentration and temperature were found to be effective on the adsorption process. Thermodynamic parameters $\Delta G^o$, $\Delta H^o$ and $\Delta S^o$ showed the endothermic and spontaneous nature of the adsorption of Pb(II) and Cd(II) ions onto $TiO_2$/kaolinite nanocomposite. Langmuir model showed the best fit for the experimental data. The maximum adsorption capacity (qmax) of Pb(II) and Cd(II) ions onto $TiO_2$/kaolinie nanocomposite at pH 6.0 and 30°C is 333.33mg/g for Pb(II) ions and 250mg/g for Cd(II) ions. Compared to various adsorbents reported in the literature, the $TiO_2$/kaolinite nanocomposite showed good promise for its use in water and wastewater treatments.

**Table 3:** Maximum adsorption capacity $q_{max}$ (mg/g) for Pb(II) and Cd(II) ions and the published values in literature

| Adsorbents | Pb(II) | Cd(II) | References |
|---|---|---|---|
| Natural kaolin clay | 2.35 | 0.88 | Jiang et al. (2010) |
| Kaolinite | 11.5 | 6.8 | Gupta and Bhattacharyya (2008) |
| Montmorillinite | 31.1 | 30.7 | Gupta and Bhattacharyya (2008) |
| Kaolinite/Smectite natural | 0.78 | | El-Naggar et al. (2019) |
| Ball clay | | 27.17 | Rao & Kashifuddin (2016) |
| Montmorillinite | | 6.98 | de Pablo et al. (2011) |
| Nanoplatelets kaolinite | 175.44 | | Al-a'qarbeh et al. (2020) |
| Tripolyphosphate impregnated kaolinite clay | 88.5 | 53.48 | Unuabonah et al. (2007) |
| Grafting kaolinite with dietthanolamiine | 45.87 | 31.45 | Koteja and Matusik (2015) |
| Grafting kaolinite with triethanolamine | 30.21 | 23.26 | Koteja and Matusik (2015) |
| polyphosphate-modified kaolinite clay | 40 | 13.23 | Amer et al. (2010) |
| Acid-modified monmorillinite | 1.62 | 0.62 | Akpomie and Dawadu (2016) |
| A novel nano-clay | 56.18 | 41.67 | Unuabonah et al. (2008) |
| NanoIllite/smectite clay | 2.56 | | Yin et al. (2018) |
| Kaolinite | 87.26 | 35.92 | Adebowale et al. (2005) |
| Phosphate-modified kaolin | 93.28 | 61.44 | Adebowale et al. (2005) |
| Sulfate -modified kaolin | 89.08 | 42.57 | Adebowale et al. (2005) |
| Kaolinite clay | 25.32 | 22.38 | Ogbu et al. (2019) |
| Sawdust-clay modified | 37.98 | 36.36 | Ogbu et al. (2019) |
| $TiO_2$/kaolinite nanocomposite | 333.33 | 250 | This work |

**ACKNOWLEDGEMENTS**

Authors are thankful to Royal Scientific Society and the University of Jordan, Jordan for providing the necessary facilities to carry out this work.

**REFERENCES**

Adebowale, K.O., Unuabonah, I.E., Olu-Owolabi, B.I., 2005. Adsorption of some heavy metal ions on sulfate- and phosphate-modified kaolin. Applied Clay Science 29, 145-148.

Akbal, F., Camcl, S., 2011. Copper, chromium and nickel removal from metal plating wastewater by electrocoagulation. Desalination 269,214–222.

Akpomie, K.G., Dawodu, F.A., 2016. Acid-modified montmorillonite for sorption of heavy metals from automobile effluent. Beni-Suef University Journal of Basic and Applied Sciences 5, 1–12.

Alasadi, A.M., Khaili, F.I., Awwad, A.M., 2019. Adsorption of Cu(II), Ni(II) and Zn(II) ions by nano kaolinite: Thermodynamics and kinetics studies. Chemistry International 5, 258-268.

Al-a'qarbeh, M.M., Shammout, M.W., Akl M. Awwad, A.M., 2020. Nano platelets kaolinite for the adsorption of toxic metal ions in the environment. Chemistry International 6, 49-55.

Al-Dujaili, A.H., Awwad, A.M., Salem, N.M., 2012. Biosorption of cadmium (II) onto loquat leaves (*Eriobotrya japonica*) and their ash from aqueous solution, equilibrium, kinetics, and thermodynamic studies. International Journal of Industrial Chemistry 3, 22.

Al-Qahtani, K.M., 2017. Cadmium removal from aqueous solution by green synthesis zero valent silver nanoparticles with Benjamina leaves extract. Egyptian Journal of Aquatic Research 43, 269–274.

Amer, M.A., Awwad, A.M., 2017. Removal of Zn(II), Cd(II) and Cu(II) ions from aqueous soliution by nano-structured kaolinite. Asian Journal of Chemistry 29, 965-969.

Amer, M.W., Ahmad, R.A., Awwad, A.M., 2015. Biosorption of Cu(II), Ni(II), Zn(II) and Pb(II) ions from aqueous solution by *Sophora japonica* pods powder. International Journal of Industrial Chemistry 67–75.

Awwad, A.M., Salem, N.M., Ahmad, A.R., 2010. Biosorption of Cr(VI) onto loquat bark from aqueous solution. Environmental Science 5, 5–11.

Banerjee, S.S., Chen, D-H., 2007. Fast removal of copper ions by gum Arabic modified magnetic nano-adsorbent. Journal of Hazardous Materials 147, 792–799.

Boudrahem, F., Aissani-Benissad, F., Soualah, A., 2011. Adsorption of Lead(II) from aqueous solution by using leaves of date trees as an adsorbent. Journal of Chemical and Engineering Data 56, 1804-1808.

Cao, C.-Y., Qu, J., Yan, W.-S., Zhu, J.-F., Wu Z.-Y., Song, W.-G., 2012. Low-cost synthesis of flowerlike α-$Fe_2O_3$ nanostructures for heavy metal ion removal: Adsorption property and mechanism. Langmuir 28, 4573-4579.

Choi, S., Jeong, Y., 2008. The Removal of heavy metals in aqueous solution by hydroxyapatite/cellulose composite. Fibres and Polymers 9, 267-270.

De bablo, L., Chavez, M.L., Abatal, M., 2011. Adsorption of heavy metals in acid to alkaline environments by montmorillonite and Ca-montmorliinite. Chemical Engineering Journal 171, 1276-286.

Bhatia, P., Nath, M., 2020. Green synthesis of p-NiO/n-ZnO nanocomposites: Excellent adsorbent for removal of congo red and efficient catalyst for reduction of 4-nitrophenol present in wastewater. Journal of Water Process Engineering 33, 101017.

Chen, D., Sun, H., Wang, Y., Quan, H., Ruan, Z., Ren, Z., Luo, X., 2020. UiO-66 derived zirconia/porous carbon nanocomposites for efficient removal of carbamazepine and adsorption mechanism. Applied Surface Science 507, 145054.

Chowdhury, A., Kumari, S., Khan, A.A., Hussain, S., 2020. Selective removal of anionic dyes with exceptionally high adsorption capacity and removal of dichromate ($Cr_2O_7^{2-}$) anion using Ni-Co-S/CTAB nanocomposites and its adsorption mechanism. Journal of Hazardous Materials 385, 121602.

D'Cruz, B., Madkour, M., Amin, M.O., Al-Hetlani, E., 2020. Efficient and recoverable magnetic AC-$Fe_3O_4$ nanocomposite for rapid removal of promazine from wastewater. Materials Chemistry and Physics 240, 122109.

Dube, D., Chingoma, C., 2016. Removal of heavy metal ions from household drinking water using *Acacia galpinii* seeds and seed pods. Journal of Health and Pollution 6, 7–14.

Elfeky, S.A., Mahmoud, S.E., Youssef, A.F., 2017. Applications of CTAB modified magnetic nanoparticles for removal of chromium (VI) from contaminated water. Journal of Advanced Research 8, 435–443.

El-Naggar, I.M., Ahmed, S.A., Shehata, N., Sheneshen, E.S., Fathy, M., Shehata, A., 2019. A novel approach for the removal of lead(II) ion from wastewater using kaolinite/smectite natural composite adsorbent. Applied Water Science 9:7.

Farhan, A. M., Al-Dujaili, A.H., Awwad, A.M., 2013. Equilibrium and kinetic studies of cadmium(II) and lead(II) ions biosorption onto *Ficus carcia* leaves. International Journal of Industrial Chemistry 4, 24.

Freundlich, H.M.F., 1906. Uber die adsorption in losungen. Zeitschrift fuer Physikalische Chemie 1906*, 57: 385–470.*

Fu, Y., Liu, X., Chen, G., 2019. Adsorption of heavy metal sewage on nano-materials such as titanate/$TiO_2$ added lignin. Results in Physics 12, 405–411.

Ge, F., Li, M.-M., Ye, H., Zhao, B.-X., 2012. Effective removal of heavy metal ions $Cd^{2+}$, $Zn^{2+}$, $Pb^{2+}$, $Cu^{2+}$ from aqueous solution by polymer-modified magnetic nanoparticles. Journal of Hazardous Materials 211-212, 366-372.

Ghorbani, M., Seyedin, O., Aghamohammadhassan, M., 2020. Adsorptive removal of lead (II) ion from water and wastewater media using carbon-based nanomaterials as

unique sorbents: A review. Journal of Environmental Management 254, 109814.

González-Muñoz, M.J., Rodríguez, M.A., Luque, S., Álvarez, J.R., 2006. Recovery of heavy metals from metal industry waste waters by chemical precipitation and nanofiltration. Desalination 200, 742–744.

Grover, V. A., Hu, J., Engates, K. E., Shipley, H. J., 2012. Adsorption and desorption of bivalent metals to hematite nanoparticles. Environmental Toxicology and Chemistry 31, 86-92.

Gupta, S., Kumar, A., 2019. Removal of nickel (II) from aqueous solution by biosorption on *A. barbadensis* Miller waste leaves powder. Applied Water Science 9, 96.

Gupta, S.S., Bhattacharyya, K,G., 2008. Immobilization of Pb(II), Cd(II) and Ni(II) ions on kaolinite and montmorillinote surfaces from aqueous medium. Journal of Environmental Management 87, 46-58.

Gupta, V.K., Agarwal, S., Saleh, T.A., 2011. Synthesis and characterization of alumina-coated carbon nanotubes and their application for lead removal. Journal of Hazardous Material 185, 17-21.

Hevira, L., Munaf, E., Zein, R., 2015. The use of *terminalia catappa* L. Fruit shell as biosorbent for the removal of Pb(II), Cd(II) and Cu(II) ion in liquid waste. Journal of Chemical and Pharmaceutical Research 7, 79-89.

Hossain, M. A. H., Haongo, G.O., Guo, W. S., Nguaen, T. V., 2012. Removal of copper from water by adsorption onto banana peel as bioadsorbent. International Journal of Geomate 2, 227-332.

Huang, L., He, M., Chen, B., Hu, B., 2018. Magnetic Zr-MOFs nanocomposites for rapid removal of heavy metal ions and dyes from water. Chemosphere 199, 435-444.

Jafarinejad, S., Faraji, M., Norouzi, Z., Mokhtari-Aliabad, J., 2018. Application of sulfur-modified magnetic nanoparticles for cadmium removal from aqueous solutions. Journal of Water and Environmental Nanotechnology 3, 58-69.

Jiang, M-q., Jin, X-y., Lu, X-Q., Chen, Z-l., 2010. Adsorption ofPb(II), Cd(II), Ni(II) and Cu(II) onto natural kaolinite clay. Desalination 252, 33-39.

Jin, Y., Liu, F., Tong, M., 2012. Modified magnetic nanoparticles. Journal of Hazardous Materials 227–228, 461– 468.

Kamari, S., Shahbazi, A., 2020. Biocompatible $Fe_3O_4$@$SiO_2$-$NH_2$ nanocomposite as a green nanofiller embedded in PES–nanofiltration membrane matrix for salts, heavy metal ion and dye removal: Long–term operation and reusability tests. Chemosphere 243, 125282.

Kefeni, K.K., Mamba, B.B., 2020. Photocatalytic application of spinel ferrite nanoparticles and nanocomposites in wastewater treatment: Review. Sustainable Materials and Technologies 23, e00140.

Koteja, A., Matusik, J., 2015. Di- and triethanolamine grafted kaolinite of different structure order adsorbent of heavy metals. Journal of Colloid and Interface Science 455, 83-92.

Langmuir, I., 1918. The adsorption of gases on plane surfaces of glass, mica and platinum. Journal of the American Chemical Society 40, 1361–1402.

Lei, Y., Chen, F., Luo, Y., Zhang, L., 2014. Three-dimensional magnetic graphene oxide foam/$Fe_3O_4$ nanocomposite as an efficient absorbent for Cr(VI) removal. Journal of Materials Science 49, 4236-4245.

Liu J.-F., Zhao, Z.-S., Jiang G.-B., 2008. Coating $Fe_3O_4$ magnetic nanoparticles with humic acid for high efficient removal of heavy metals in water. Environmental Science and Technology 42, 6949-6954.

Luo, X., Lei, X., Cai, N., Xie, X., Xue, Y., Yu, F., 2016. Removal of heavy metal ions from water by magnetic cellulose-based beads with embedded chemically modified magnetite nanoparticles and activated carbon. ACS Sustainable Chemistry and Engineering 47, 3960-3969.

Mahmoud, M.E., Fekry, N.A., El-Latif, M.M.A., 2016. Nanocomposites of nanosilica-immobilized-nanopolyaniline and crosslinked nanopolyaniline for removal of heavy metals. Chemical Engineering Journal 304, 679–691.

Martinez, M., Miralles, N., Hidalgo, S., Poch, J., 2006. Removal of lead(II) and cadmium(II) from aqueous solutions using grape stalk waste. Journal of Hazardous Materials 133, 203-211.

Mavrov, V., Erwe, T., Blöcher, C., Chmiel, H., 2003. Study of new integrated processes combining adsorption, membrane separation and flotation for heavy metal removal from wastewater. Desalination 157, 97–104.

Mukwevho, N., Gusain, R., Fosso-Kankeu, E., Kumar, N., Waanders, F., Ray, S.S., 2020. Removal of naphthalene from simulated wastewater through adsorption-photodegradation by ZnO/Ag/GO nanocomposite. Journal of Industrial and Engineering Chemistry 81, 393-404.

Ogbu, L.C., Akpomie, K.G., Osunkunle, A.A., Eze, S.I., 2019. Sawdust-kaolinite composite as efficient sorbent for heavy metal ions. Bangladesh Journal of Scientific and Industrial Research 54, 99-110.

Ojemaye, M.O., Okoh, O.O., Okoh, A.I., 2017. Surface modified magnetic nanoparticles as efficient adsorbents for heavy metal removal from wastewater: Progress and prospects. Materials Express 7, 439-456.

Oluwaseun, A., Amoo, I.A., Abiodun, A., 2011. Biosorption of Lead (II) ions from aqueous solution using *Moringa oleifera* pods. Archives of Applied Science Research 3, 50-60.

Pan, L., Wang, Z., Yang, Q., Huang, R., 2018. Efficient removal of lead, copper and cadmium ions from water by a porous calcium alginate/graphene oxide composite aerogel. Nanomaterials 8, 957.

Rao, R.A.K., Kashifuddin, A., 2016. Adsorption studies of Cd(II) on ball clay: Comparison with other natural clays. Arabian Journal of Chemistry 9, S1233–S1241.

Roy, A., Bhattacharya, J., 2012. Removal of Cu(II), Zn(II) and Pb(II) from water using microwave-assisted synthesized

maghemite nanotubes. Chemical Engineering Journal 211-212, 493-500.

Roy, A., Bhattacharya, J., 2013. A binary and ternary adsorption study of wastewater Cd(II), Ni(II) and Co(II) by γ-$Fe_2O_3$ nanotubes. Separation and Purification Technology 115, 172-179.

Saeedi-Jurkuyeh, A., Jafari, A.J., Kalantary, R.R., Esrafili, A., 2020. A novel synthetic thin-film nanocomposite forward osmosis membrane modified by graphene oxide and polyethylene glycol for heavy metals removal from aqueous solutions. Reactive and Functional Polymers 146, 104397.

Schwantes, D., Gonçalves, A.C., De Varennes, A., Braccini, A.L., 2018. Modified grape stem as a renewable adsorbent for cadmium removal. Water Science and Technology 78, 2308-2320.

Shahzad, A., Jang, J., Lim, S.-R., Lee, D.S., 2020. Unique selectivity and rapid uptake of molybdenum-disulfide-functionalized MXene nanocomposite for mercury adsorption. Environmental Research 182, 109005.

Sheet, I., Kabbani, A., Holail, H., 2014. Removal of heavy metals using nanostructured graphite oxide, silica nanoparticles and silica/ graphite oxide composite. Energy Procedia 50, 130 - 138.

Sheydaei, M., Soleimani, D., Ayoubi-Feiz, B., 2020. Simultaneous immobilization of Dy2O3, graphite and $TiO_2$ to prepare stable nanocomposite for visible light assisted photocatalytic ozonation of a wastewater: Modeling via artificial neural network. Environmental Technology and Innovation 17, 100512.

Şölener, M., Tunali, S., Özcan, A.S., Özcan, A., Gedikbey T., 2008. Adsorption characteristics of lead(II) ions onto the clay/poly(methoxyethyl)acrylamide. Desalination 223, 308-322.

Song, J., Kong, H., Jang, J., 2011. Adsorption of heavy metal ions from aqueous solution by polyrhodanine-encapsulated magnetic nanoparticles. Journal of Colloid and Interface Science 359, 505-511.

Sudilovskiy, P.S., Kagramanov, G.G., Trushin, A.M., Kolesnikov, V.A., 2007. Use of membranes for heavy metal cationic wastewater treatment: Flotation and membrane filtration. Clean Technologies and Environmental Policy 9, 189-198.

Tan, L., Xu, J., Xue, X., Lou, Z., Zhu, J., Baig, S. A., Xu, X., 2014. Multifunctional nanocomposite $Fe_3O_4$@$SiO_2$-mPD/SP for selective removal of Pb(II) and Cr(VI) from aqueous solutions. RSC Advances 86, 45920-45929.

Taseidifar, M., Makavipour, F., Pashley, R.M., Rahman, A.F.M.M., 2017. Removal of heavy metal ions from water using ion flotation. Environmental Technology and Innovation 8, 182-190.

Tinas, T., Caliskan, E., Kan A, Ozbek N, Akman S., 2016. Preparation of $Fe_3O_4$@montmorillonite composite as an effective sorbent for the removal of lead and cadmium from wastewater samples. Turkish Journal of Chemistry 40, 974- 978.

Tran, T.K., Leu, H.J., Chiu, K.F., Lin, C.Y., 2017. Electrochemical treatment of heavy metal-containing wastewater with the removal of COD and heavy metal Ions: Electrochemical treatment of heavy metal containing wastewater. Journal of the Chinese Chemical Society 64, 493–502.

Unuabonah, E.I., Olu-Owolabi, B.I, Adebowale, K.O., Yang L.Z., 2008. Removal of lead and cadmium ions from aqueous solution by polyvinyl alcohol-modified kaolinite clay: A Novel nano-clay dsorbent. Adsorption Science and Technology 26, 383-405.

Unuabonah, E.I., Olu-Owolabi, B.I., Adebowale, K.O., Ofomaja, A.E., 2007. Adsorption of lead and cadmium ions from aqueous solutions by tripolyphosphate-impregnated kaolinite clay. Colloids and Surfaces A: Physicochemical and Engineering Aspects 292, 202-211.

Verbych, S., Hilal, N., Sorokin, G., Leaper, M., 2004. Ion exchange extraction of heavy metal ions from wastewater. Separation and Purification Technology 39, 2031–2040.

Wang, X., Guo, Y., Yang, L., Han, M., Zhao, J., Cheng, X., 2012. Nanomaterials as sorbents to remove heavy metal ions in wastewater treatment. Journal of Environmental and Analytical Toxicology 2, 154.

Wang, Y., Cheng, R., Wena, Z., Zhao, L., 2012. Facile preparation of $Fe_3O_4$ nanoparticles with cetyltrimethylammonium bromide (CTAB) assistant and a study of its adsorption capacity. Chemical Engineering Journal 181–182, 823– 827.

Wang, Y., Cheng, R., Wena, Z., Zhao, L., 2012. Facile preparation of $Fe_3O_4$ nanoparticles with cetyltrimethylammonium bromide (CTAB) assistant and a study of its adsorption capacity. Chemical Engineering Journal 181-182, 823-827.

Yang, J., Hou, B., Wang, J., Tian, B., Bi, J., Wang, N., Li, X., Huang, X., 2019. Nanomaterials for the removal of heavy metals from wastewater. Nanomaterials 9, 424.

Yin, J., Deng, C., Yu, Z., Wang, X., Xu, G., 2018. Effective removal of lead ions from aqueous solution using nanoIllite/Smectite clay: isotherm, kinetic and thermodynamic modeling of adsorption. Water 10, 210.

Yue, Y., Zhang, P., Wang, W., Cai, Y., Tan, F., Wang, X., Qiao, X., Wong, P.K., 2020. Enhanced dark adsorption and visible-light-driven photocatalytic properties of narrower-band-gap $Cu_2S$ decorated $Cu_2O$ nanocomposites for efficient removal of organic pollutants. Journal of Hazardous Materials 384, 121302.

Zhang, Z., He, S., Zhang, Y., Zhang, K., Wang, J., Jing, R., Yang, X., Hu, Z., Li, Y., 2019. Spectroscopic investigation of $Cu^{2+}$, $Pb^{2+}$ and $Cd^{2+}$ adsorption behavior by chitosan-coated agrillaceow limestone: Comparison and mechanism. Environmental Pollution 254, 112938.